Initial Assessment of Dye Incorporation in *Bombyx mori* Silk Biomaterials

Cindy Gu
Basis Independent Fremont
Newark, USA
cindyisawesome36@gmail.com

James Gu
Stanford University
Stanford, USA
jamesgu8@stanford.edu

***Abstract*—This study presents a preliminary and environmentally sustainable method for producing fluorescent silk by incorporating fluorescent dyes directly into the diet of *Bombyx mori* silkworms. Five dye compounds—Fluorescein Sodium, Rhodamine B, Rhodamine 101 Inner Salt, Sulforhodamine 101, and Rhodamine 110 Chloride—were administered at a 0.1% concentration (0.02 g of dye per 20 g of mulberry chow) starting at the 2nd instar. Silk cocoons formed during the 5th instar were analyzed for fluorescence, mechanical strength, and structural consistency. Rhodamine B exhibited the highest fluorescence intensity, followed by Sulforhodamine 101, Rhodamine 101 Inner Salt, Fluorescein Sodium, and Rhodamine 110 Chloride. Tensile strength testing revealed the control group had the highest mechanical strength, with strength decreasing in the following order: Sulforhodamine 101, Rhodamine 101 Inner Salt, Rhodamine 110 Chloride, Fluorescein Sodium, and Rhodamine B. Optical microscopy showed uniform silk structure in the control group, semi-uniformity in Sulforhodamine 101, Rhodamine B, and Rhodamine 101 Inner Salt, with inconsistency in Rhodamine 110 Chloride and Fluorescein Sodium. This method of producing fluorescent silk eliminates the need for post-processing while preserving mechanical integrity and enabling stable long-term fluorescence. The resulting biocompatible silk materials hold strong potential in clinical biosensing applications, where implantable silk fibers serve as real-time monitors of disease markers, infection, or wound healing progression through visible fluorescence changes, offering a natural, safe, and flexible alternative for in vivo diagnostics and regenerative therapies.**

Keywords*—*Fluorescent silk, organic dyes, Bombyx mori, biosensors, biocompatible materials, dietary dye incorporation, silk fibroin

I. Introduction

Silk fibroin, the primary structural protein in silk, is valued for its exceptional biocompatibility, biodegradability, mechanical strength, optical clarity, and biological versatility [1]. These properties make it highly suitable for a range of biomedical applications, such as tissue engineering, drug delivery, cancer therapy, and the regeneration of skin, bone, and ocular tissues [1]. Fluorescent silk, engineered to emit light under ultraviolet or other electromagnetic radiation, can be processed into sponges, hydrogels, 2D/3D films, fibroin mats, and fibers for various medical uses [2]. Notably, silk fibroin can maintain stable fluorescence over extended periods of time, supporting its use in biocompatible and long-term applications [3]. In tissue engineering, silk also facilitates cell adhesion and growth, making it a promising scaffold material for tissue regeneration [4].

Fluorescent silk has been used as a biosensor and marker in biomedical imaging. When embedded with fluorescent dyes, it enables visualization of tissue growth, monitoring of wound healing, and tracking of the distribution of drugs and cells in the body [2]. Fluorescent silk has also been developed as scaffolding in tissue engineering, which can help provide structural support for cell growth and the fluorescent properties can help track the process [3]. Fluorescent silk fibroin retains stable fluorescence for up to a year, making it suitable for long term medical monitoring and implants [4]. Overall, its optical properties make it valuable for monitoring biological processes and guiding tissue development [5]. Due to its porous 3D structure, it can be engineered to become scaffolds, which can be used for several different purposes specifically for bone regeneration and skin tissue repair [6].

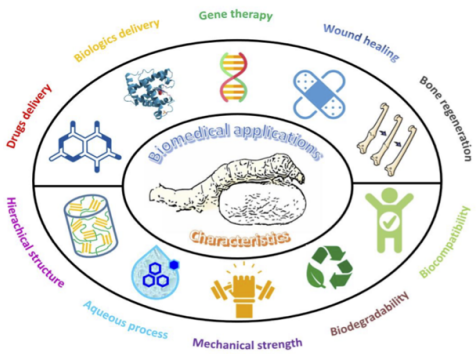

Figure 1: Examples of applications of silk used in the biomedical field [6].

Recent studies have emphasized the biomedical applications of *Bombyx mori* silk through both in vitro and in vivo analyses. In one such study, Chen et al. explored the incorporation of quercetin, a naturally fluorescent and antioxidant compound, into silk fibroin through dietary supplementation of the silkworms, followed by evaluation of growing mouse fibroblast on the resulting scaffolds [7]. A group of 320 healthy silkworms were divided into four groups with different quercetin concentrations, and monitored for health status and survival outcomes [7]. At the fifth instar stage, silk glands were rinsed and examined via hematoxylin and eosin staining, after which cocoons were degummed with sodium carbonate (Na_2CO_3) and processed into scaffolds [7]. Mouse fibroblast culture studies demonstrated effective cell adhesion and minimal apoptosis, confirming the cytocompatibility and non-toxic nature of the quercetin silk scaffolds [7]. Genetic modification and selective breeding of such silkworms have also

improved silk yield, purity, and structural properties as well to allow scientists to fabricate scaffolds that most similarly match natural tissues [8]. This can further allow for the silk to be made into a more adhesive and beneficial silk scaffold.

Another study uses in vitro tests on testing the biocompatibility of knitted silk fibroin scaffolds made from non-mulberry silk fibroin, and investigating cell growth and regeneration from these tissue-engineered biomaterials [9]. Their study focuses on the clinical challenge of rotator cuff tendon tears, as Musson et al. investigated Spidrex®, a new scaffold made from non-mulberry silk fibroin to see if it could support tendon repair [9]. Synthetic and natural biomaterials have emerged as promising alternatives in tissue engineering as they can be designed to mimic the physical, chemical, and biological properties of native tissues [8]. The human and rat tenocytes attached to Spidrex® grew more in number over 14 days, and under gene testing Spidrex® had higher expression of tendon-related genes and lower expression of genes linked with cartilage or bone cells [9].

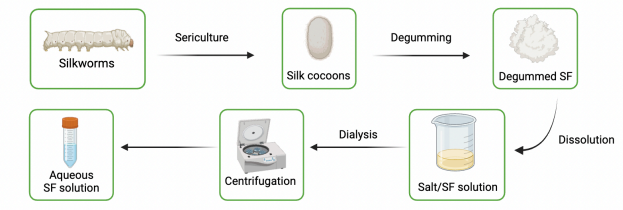

Figure 2: Process of degumming a silk cocoon from a silkworm into an Aqueous Silk Fibroin solution. Created using Biorender.com

Through using in vivo tests on investigated self-assembling silk fibroin hydrogels from *Bombyx mori* for promoting tissue repair, Gorenkova et al. inspects the biocompatibility and interaction in experimental strokes on rats [10]. Using a transient middle cerebral artery occlusion model, 24 Sprague-Dawley rats underwent focal ischemic injury, and were injected with a Phosphate-buffered saline or an injection of 4% w/v fibroin hydrogels to be observed for neurological impact and body weight [10]. Immunofluorescence staining showed the hydrogel interacted with but did not disrupt with the surrounding astrocytes, and the hydrogel structure provided a supportive microenvironment for cellular proliferation as a minimally invasive biomaterial for enhancing post-stroke brain repair [10].

Yigit et al. checks for mutagenicity and genotoxicity by running the Ames bacterial reverse mutation test and an in vivo mouse micronucleus assay to detect whether a substance can damage DNA [11]. Silk fibroin is a solution tested as it is highly biocompatible, exhibits remarkable mechanical properties, and can be processed into various forms such as films, fibers, hydrogels, or composites [8]. To examine systemic toxicity, they conducted a 14-day and 28-day feeding study in rats, where they fed rats a silk fibroin solution and monitored their body weight, blood markers, and overall health [11]. Silk fibroin showed no toxic effects in rats even at the maximum soluble dose (500-1000 mg/kg/day), which supports SF's thermal safety for biomedical use [11]. There were no signs of mutagenic or genotoxic activity, showing SF does not cause any DNA damage under chemical or metabolic stress [11].

In the study from Pang et al., researchers fabricated fluorescent silk fibroin nanofibers using electrospinning with three dyes, Fluorescein Sodium, Rhodamine B, and Acridine orange [12]. Structural analyses showed that the dyes did not alter the silk fibroin's structure, and thermal degradation consistently began around 250 °C [12].

Additionally, Yamane et al. studied the structural organization of *Bombyx mori* silk fibroin in its unspun silk, and simulated three dipeptides, Ac-Gly-NHMe, Ac-Ala-NHMe, and Ac-SerNHMe in water to understand the crystalline regions of fibroin [13]. From these data, they constructed conformational probability maps on the Ramachandran plane, and showed that the dipeptides form stable shapes of type II β-turns [13]. This supported the idea that silk fibroin in its unspun form is made of repeated β-turns structures, and found that some β-turns stayed stable while others shifted into looser, coil-like shapes which showed that the structure is flexible in water [13].

This study builds upon prior research exploring environmentally friendly methods of producing modified silk using silkworms. Wu et al. reviewed the potential of naturally modified silk as a sustainable alternative to synthetic production, emphasizing its direct biosynthesis by silkworms [2]. Xiong et al. developed a safe and innovative technique using red carbon dots extracted from mulberry leaves to induce fluorescence in silk, demonstrating biocompatibility and non-toxicity to the silkworms [14]. Similarly, Ahmed et al. investigated eco-conscious approaches by feeding dyed mulberry leaves, reducing reliance on post-processing dyeing methods, which are typically costly and environmentally harmful [15]. Additionally, Ramos et al. showed that incorporating nanomaterials into the silkworms' diets could enhance the resulting silk fibers' properties without exposing the silkworms to toxic chemicals [16]. These studies collectively highlight the feasibility and environmental advantages of modifying silk during the silkworm rearing process.

Although prior studies have advanced the development of fluorescent silk, key research gaps remain. Tansil et al. demonstrated the production of fluorescent silk and its subsequent reeling and purification into fibroin segments [17], and further investigated how xenobiotics, foreign compounds, are metabolized within the silkworm body [18]. However, there has been no comprehensive study comparing different fluorescent dyes and their effects on both silk properties and silkworm health. This study addresses this gap by evaluating multiple Rhodamine-based and other fluorescent dyes, analyzing their impact on silk using tensile strength measurements and optical microscopy. Additionally, the physiological response of silkworms to each dye is assessed by observing body coloration and fluorescence under visible and 365 nm ultraviolet (UV) light. Lastly, this study compares two environmentally sustainable delivery methods, dyed mulberry leaves and mulberry chow, to determine the most effective approach for incorporating fluorescent dyes into silkworm diet.

II. Methodology

A. Different Types of Fluorescent Dyes

The dye materials used in this experiment were organic, non-nanomaterial dyes, including Rhodamine 101 Inner Salt, Rhodamine 123, Rhodamine 6G, Rhodamine B, Sulforhodamine 101, Acridine Orange, and Fluorescein Sodium (Sigma Aldrich).

B. Raising Silkworms

Silkworms were raised at a controlled temperature of 24-29°C, optimal for their growth and cocoon production. In this experiment, the initial batch was first fed fresh mulberry leaves and later transitioned to silkworm chow to improve dye incorporation. The first group served as the control and received no fluorescent dyes. Beginning with the second batch, various fluorescent dyes were mixed into their diet, and the silkworms were monitored for physiological and silk-related changes. Fluorescent dyes were incorporated into reconstituted mulberry chow at a final concentration of 0.1% (w/w). Specifically, 0.02 g of dye powder was thoroughly mixed into 20 g of hydrated chow before feeding. This equates to ~1 mg of dye per gram of feed. Based on average consumption of 3–5 g of chow per larva per day at the fifth instar, each larva ingested approximately 3–5 mg of dye daily.

Silkworms are invertebrates and are not subject to Institutional Animal Care and Use Committee or equivalent ethical review under current U.S. regulations. Nevertheless, all rearing and experimental procedures were conducted under humane and non-invasive conditions, ensuring no unnecessary harm to the organisms.

C. Mechanical Properties

To evaluate the mechanical properties of the silk, tensile strength testing was performed using a spring scale to measure the maximum load that each silk sample could withstand. Each silk scaffold was cut into standardized strips measuring 3 cm in length and 2 cm in width. The sample was looped around the hook of the calibrated spring scale and pulled downward until the scale locked, indicating the maximum force the silk could tolerate before failure. This procedure was repeated ten times per sample to ensure consistency and to generate a more robust dataset, which was then used to compare the tensile strength across different dye-treated groups.

III. Results and Discussion

The lifecycle progression of *Bombyx mori* is critical to understanding when dye exposure is most effective. As illustrated in Fig. 3, the full lifecycle spans approximately 45-50 days, beginning with the egg stage (Fig. 3A). By day 5, the larvae enter the 1st instar (Fig. 3B), feeding on the edges of mulberry leaves. Around day 9 (Fig. 3C), they molt into the 2nd instar, growing to about 2 cm in length. At this stage, the silkworms were divided into equal groups and placed in separate enclosures to receive different fluorescent dye treatments. By day 30, they reach the 4th to 5th instar stage (Fig. 3D), growing to approximately 2.54 cm in length. During the 5th instar, the silkworms begin spinning cocoons, at which point the

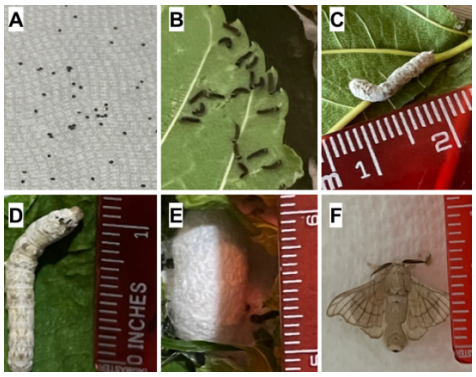

Figure 3: Silkworm life cycle. A) silkworm eggs; B) silkworm on day 5 (1st instar); C) silkworm on day 9 (2nd instar); D) silkworm on day 30 (4th and 5th instar); E) silkworm cocoon day 30; and F) silk moth

fluorescent dyes became visible in the silk. Fig. 3E shows a completed cocoon, where the silkworm pupates until it emerges as a moth around day 50 (Fig. 3F).

A total of 200 silkworms were utilized in this study. The specimens were divided into six experimental groups of 33 individuals each, corresponding to the different fluorescent dye treatments, and one control group. The remaining two silkworms were allocated to the control group to balance sample size. During the first and second instar stages, all groups were maintained on standard silkworm chow to ensure acclimation to the rearing environment and to promote survival. Beginning at the third instar, the experimental groups received chow supplemented with the assigned fluorescent dyes, while the control group continued to receive unaltered chow. Five silkworms were randomly selected from each group daily and assessed for behavioral and physiological indicators, including movement activity and body coloration. All silkworms from each group showed no significant behavioral changes and survived until adulthood, which showed there are no harmful effects on adding fluorescent dyes into their chow.

To assess dye fluorescence, Fig. 4 presents organic fluorescent dyes under both room and UV lighting. In Fig. 4A, the dyes are shown under room lighting, where each exhibits strong color saturation. Among them, Sulforhodamine 101 appears the lightest, with a pale pink hue. Fig. 4B presents the same dyes under 365 nm UV light, where all mixtures demonstrate high fluorescence, confirming their suitability for dietary incorporation. Each dye was used in powder form, with 0.02 g mixed into 20 g of mulberry chow to achieve a 0.1% concentration. Only Rhodamine B, Sulforhodamine 101, and Rhodamine 101 Inner Salt produced visible fluorescence in the silkworms themselves. Of these three, only Rhodamine B and Sulforhodamine 101 also resulted in visibly fluorescent cocoons. Recent studies have also tested the fluorescence of other materials, such as Quercetin, which was found to be able to produce a stable fluorescence as well as enhanced antioxidant properties that allowed the silk to maintain good mechanical strength and biocompatibility [12].

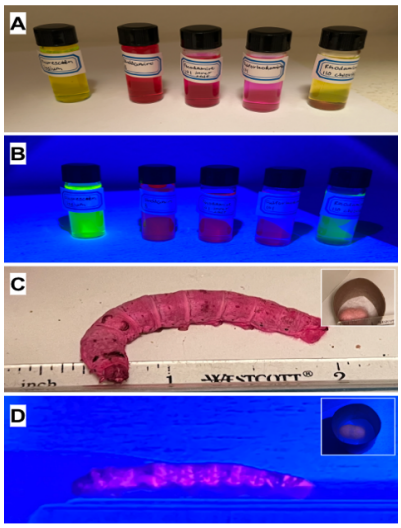

Figure 4: A-B) Fluorescent mixture under room lighting on top and UV lighting on bottom (Fluorescein Sodium, Rhodamine B, Rhodamine 101 Inner Salt, Sulforhodamine 101, Rhodamine 110 Chloride); C) Example of dyed silkworm and its cocoon of Rhodamine B dye under room light; and D) Example of Rhodamine B dyed silkworm and its cocoon under UV light

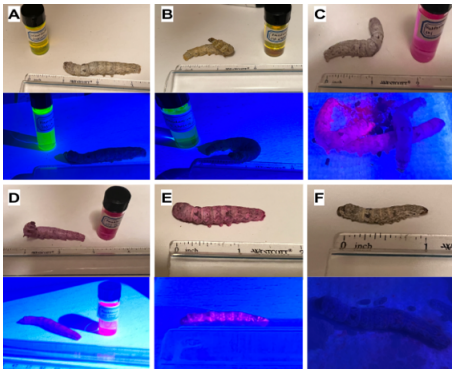

Figure 5: A-F) Different dyed silkworm under room lighting on top and under UV light (Fluorescein Sodium, Rhodamine 110 Chloride, Sulforhodamine 101, Rhodamine 101 Inner Salt, Rhodamine B, Control

Expanding on these results, Fig. 5 illustrates how the dyes affected the silkworms' appearance under room and UV lighting. The silkworms that ingested dyes with a pink hue, specifically Sulforhodamine 101, Rhodamine 101 Inner Salt, and Rhodamine B, exhibited the highest fluorescence under UV light (Figs. 4C-E), indicating effective absorption through the silkworms' digestive system. In contrast, Fluorescein Sodium and Rhodamine 110 Chloride produced strong yellow fluorescence in solution but failed to generate visible fluorescence in the silkworms themselves. As shown in Figs. 5A and 5B, these silkworms displayed no change under UV light, suggesting that the dyes were not absorbed but instead excreted as waste. The digestive tract was also dissected and observed for its fluorescence stability and absorption through another study and revealed how the dyes passed through the silkworm body and excreted as waste [2]. This highlights the importance of dye compatibility with the silkworm digestive system for success in vivo fluorescence.

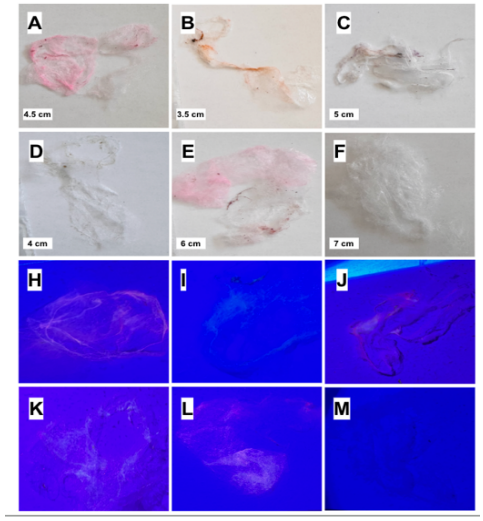

Figure 6: A-F) Silkworm silk under room light with different dye with the white bar indicating the length of each silk scaffold (Rhodamine B (pink), Rhodamine 110 Chloride (orange), Sulforhodamine 101 (purple), Fluorescein Sodium (green), Rhodamine 101 Inner Salt (pink), and Control Group); and H-M) Silk corresponding to A-F under 365 nm UV light

The impact of dye ingestion on silk is further detailed in Fig. 6, which shows silk scaffolds under both lighting conditions. When silkworms began producing silk, they were transferred to bare enclosures, allowing the silk to form directly on the sides of the container. Most scaffolds displayed visible coloration under room light and varying levels of fluorescence under UV light, though not all produced enough material to form a complete cocoon. Under room lighting, Rhodamine B (Fig. 6A) and Rhodamine 101 Inner Salt (Fig. 6E) exhibited the most intense coloration, both with a pink hue. These were followed by Rhodamine 110 Chloride (Fig. 6B) with an orange hue, Sulforhodamine 101 (Fig. 6C) with a purple hue, Fluorescein Sodium (Fig. 6D) with a green hue, and lastly the control group (Fig. 6F), which showed no coloration. Under UV lighting, Rhodamine B (Fig. 6H), Sulforhodamine 101 (Fig. 6J), and Fluorescein Sodium (Fig. 6K) demonstrated the strongest fluorescence. The observed fluorescence results from the

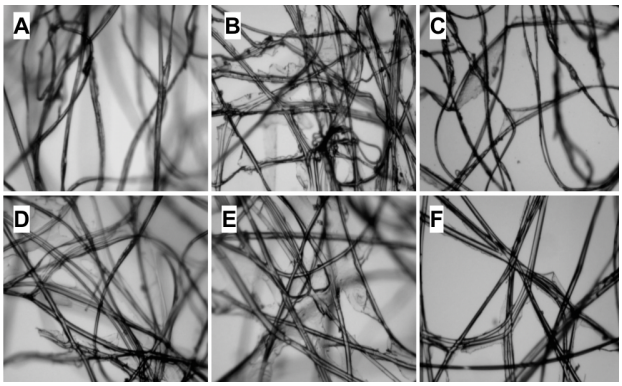

Figure 7: Different types of silk under microscope. A) Example of Sulforhodamine 101 silk; B) Example of Rhodamine 110 Chloride silk; C) Example of Fluorescein Sodium silk; D) Example of Rhodamine B silk; E) Rhodamine 101 Inner Salt silk; F) Example of Control Group silk without the addition of dyes

ingestion of dye-infused feed, where dye compounds pass through the intestinal lining and gut wall, subsequently becoming integrated into the silk as it is produced.

To analyze how dye incorporation affects fiber structure, Fig. 7 presents microscopic images of silk scaffolds under 4x objective magnification to evaluate the effects of dye incorporation on silk uniformity and mechanical properties. The control group (Fig. 7F) shows a highly uniform fiber alignment, indicating that, in the absence of dye, the silk retains its native structure. In contrast, Sulforhodamine 101 (Fig. 7A), Rhodamine B (Fig. 7D), and Rhodamine 101 Inner Salt (Fig. 7E) exhibit moderate alignment, less uniform than the control, but still directionally consistent. These deformations of the natural fiber alignment influence the silk's tensile strength and flexibility. On the other hand, Rhodamine 110 Chloride (Fig. 7B) and Fluorescein Sodium (Fig. 7C) show disorganized and irregular fiber arrangements, indicating poor integration and structural inconsistency. This lack of uniformity contributes to weakened mechanical properties, including increased brittleness and reduced tensile strength.

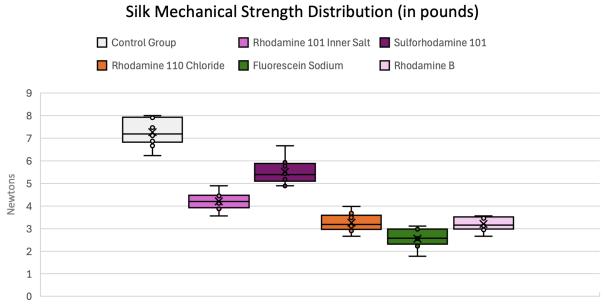

Figure 8: Whisker plot of the tensile strength of each silk scaffold in Newtons, corresponding to their color (Control Group, Rhodamine 101 Inner Salt, Sulforhodamine 101, Rhodamine 110 Chloride, Fluorescein Sodium, and Rhodamine B)

To quantify these structural observations, Fig. 8 shows the tensile strength measurements of silk scaffolds produced by silkworms fed with different fluorescent dyes. Each silk sample was tied to a spring scale and pulled downward until breaking ten times, with the maximum force (in Newtons) recorded. The control group, with a mean value of 7.27 ± SD of 0.56, demonstrated the highest tensile strength, indicating that undyed silk retains its native mechanical integrity. Sulforhodamine 101, (5.52±0.52) and Rhodamine 101 Inner Salt (4.21±0.37) also showed relatively high strength values due to being able to withstand more weight and having a higher mechanical strength distribution, suggesting minimal disruption to the silk's structural proteins during dye incorporation. In contrast, silk treated with Rhodamine 110 Chloride (3.26±0.39), Fluorescein Sodium (2.56±0.38), and Rhodamine B (3.16±0.29) exhibited significantly reduced tensile strength due to being the lowest in the distribution chart. This reduction may be attributed to interference with the assembly of fibroin and sericin, the primary structural proteins in silk. These findings suggest that certain fluorescent dyes can compromise the mechanical properties of silk.

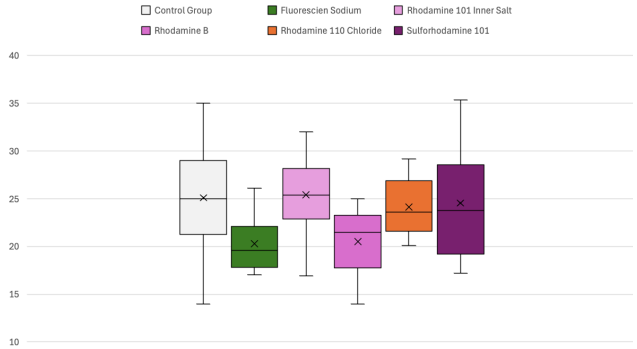

Figure 9: Box whisker plot of each silk strand diameters (in µm) of each fluorescent dye group, corresponding to their color (Control Group, Fluorescein Sodium, Rh 101 Inner Salt, Rh B, Rh 110 Chloride, Sulforhodamine 101)

To further characterize fiber morphology, strand diameters were measured from the micrographs shown in Fig. 7, and group-level results are summarized in Fig. 9. Scale bars were calibrated in micrometers (µm), and cocoon-level mean diameters were calculated from multiple strand measurements per group. The control group (with a mean value of 25.10 µm) and the Rhodamine 101 Inner Salt group (25.40 µm) exhibited the largest mean diameters, suggesting minimal structural degradation and higher resistance to mechanical stress. By contrast, Fluorescein Sodium (20.27 µm), Rhodamine B (20.50 µm), and Rhodamine 110 Chloride (20.50 µm) exhibited smaller diameters, consistent with structural weakening. Statistical comparisons to the control group confirmed that Fluorescein Sodium caused a significant reduction in diameter (p value = 0.039), while Rhodamine B (0.056), Rhodamine 110 Chloride (0.661), Sulforhodamine 101 (0.839), and Rhodamine 101 Inner Salt (0.900) did not differ significantly.

In addition to size, fiber orientation histograms (derived from Fig. 7 micrographs, not shown) were generated using ImageJ's FFT-based plugin, providing quantitative estimates of alignment angle and orientation dispersion. Groups incorporating Rhodamine B and Sulforhodamine 101 displayed broader distributions than the control, indicating reduced alignment uniformity. Taken together, the diameter and orientation analyses show that specific dyes disrupted both fiber size and structural organization, contributing to the observed reductions in mechanical performance. Future work can entail integrating sensor-based monitoring and predictive modeling into fluorescent silk systems that can enable real-time tracking of fiber formation and alignment, allowing for more precise optimization of dye incorporation and mechanical performance [20].

IV. Conclusion

The five organic fluorescent dyes evaluated in this study were chosen for their ability to produce stable, high fluorescence while preserving silk's structural integrity. Fluorescent silk scaffolds were then produced and checked for fluorescence intensity under a 365 nm UV light under visualization. The results indicated that Rhodamine B had the highest fluorescence

intensity under 365 nm UV light, followed by Sulforhodamine 101, Fluorescein Sodium, Rhodamine 101 Inner Salt, Rhodamine 110 Chloride, and finally control group having the lowest fluorescence intensity. Quantitative fiber analysis showed that groups like Rhodamine 101 Inner Salt maintained larger strand diameters (25.40 μm) and more consistent morphology, while certain dyes such as Fluorescein Sodium (20.27 μm) reduced strand size, correlating with lower mechanical performance (2.56±0.38). The mean diameter of the control group was 25.10 μm with an average tensile strength of 7.27 Newtons was the highest in both the mechanical strength as well as thickest diameter. Both values showed how the control group stayed the most intact of their silk structure, causing them to be harder and less brittle. Rhodamine B (20.50 μm) and Rhodamine 110 Chloride (20.50 μm) showed the least mean diameter, correlating to having a lower tensile strength.

Overall, these findings demonstrate that dietary dye incorporation is a practical and sustainable approach to producing fluorescent silk, establishing clear relationships between dye chemistry, fiber structure, and mechanical behavior. While spectroscopy and biocompatibility testing were beyond the scope of this initial study, future work will employ molecular-level techniques such as FTIR and Raman spectroscopy to probe how dye molecules interact with silk fibroin proteins at the β-sheet and amorphous domains. Such analyses will clarify whether reductions in tensile strength are linked to specific disruptions in fibroin secondary structures, and standardized tensile rigs can further validate these effects. Furthermore, given the long-term goal of biomedical applications, the use of near-infrared–excitable dyes could mitigate radiative safety concerns associated with UV exposure. Future work also includes adding a reference sheet to compare current silk scaffolds with a reference sheet to identify the data points of each fluorescence intensity.

By combining fluorescence enhancement with quantitative structural evaluation, this study provides a foundation for optimizing dye concentration, delivery methods, and analytical techniques. These advances will support the continued development of fluorescent silk as a versatile biomaterial with potential in biosensing, tissue engineering, and regenerative medicine.

References

[1] D. W. Kim *et al.*, "Novel fabrication of fluorescent silk utilized in biotechnological and medical applications," *Biomaterials*, vol. 70, pp. 48–56, Nov. 2015, doi: https://doi.org/10.1016/j.biomaterials.2015.08.025.

[2] Z.-F. Wu, Z.-N. Sun, and H.-M. Xiong, "Fluorescent Silk Obtained by Feeding Silkworms with Fluorescent Materials," Chin. J. Chem, vol. 41, pp. 2035–2046, 2023, doi: https://doi.org/10.1002/cjoc.202300043.

[3] K. Shimizu, "Genetic engineered color silk: Fabrication of a photonics material throuan gh a bioassisted technology," *Bioinspir. Biomim.,* 2018. [Online]. Available: https://pubmed.ncbi.nlm.nih.gov/29620530/.

[4] C. Lujerdean, G.-M. Baci, A.-A. Cucu, and D. S. Dezmirean, "The contribution of silk fibroin in biomedical engineering," *Insects*, vol. 13, no. 3, p. 286, Mar. 2022, doi: 10.3390/insects13030286.

[5] H. Xu and D. A. O'Brochta, "Advanced technologies for genetically manipulating the silkworm *Bombyx mori*, a model lepidopteran insect," *Proc. R. Soc. B Biol. Sci.*, vol. 282, no. 1810, p. 20150487, Jul. 2015, doi: https://doi.org/10.1098/rspb.2015.0487.

[6] T. P. Nguyen *et al.*, "Silk Fibroin-Based Biomaterials for Biomedical Applications: A Review," *Polymers*, vol. 11, no. 12, p. 1933, Nov. 2019, doi: https://doi.org/10.3390/polym11121933.

[7] W. Chen, G. Fu, Y. Zhong, Y. Liu, H. Yan, and F. Chen, "Antioxidant High-Fluorescent Silkworm Silk Development Based on Quercetin-Induced Luminescence," ACS Biomaterials Science & Engineering, vol. 11, no. 3, pp. 1402–1416, Feb. 2025, doi: https://doi.org/10.1021/acsbiomaterials.4c02400.

[8] G. De Giorgio et al., "Silk Fibroin Materials: Biomedical Applications and Perspectives," Bioengineering, vol. 11, no. 2, p. 167, Feb. 2024, doi: https://doi.org/10.3390/bioengineering11020167.

[9] D. S. Musson et al., "In Vitro Evaluation of a Novel Non-Mulberry Silk Scaffold for Use in Tendon Regeneration," Tissue Engineering. Part A, vol. 21, no. 9–10, pp. 1539–1551, May 2015, doi: https://doi.org/10.1089/ten.tea.2014.0128.

[10] N. Gorenkova, Ibrahim Osama, F. P. Seib, and H. V. O. Carswell, "In Vivo Evaluation of Engineered Self-Assembling Silk Fibroin Hydrogels after Intracerebral Injection in a Rat Stroke Model," ACS Biomaterials Science & Engineering, vol. 5, no. 2, pp. 859–869, Nov. 2018, doi: https://doi.org/10.1021/acsbiomaterials.8b01024.

[11] S. Yigit et al., "Toxicological assessment and food allergy of silk fibroin derived from *Bombyx mori* cocoons," Food and Chemical Toxicology, vol. 151, p. 112117, May 2021, doi: https://doi.org/10.1016/j.fct.2021.112117.

[12] L. Pang, J. Ming, F. Pan, and X. Ning, "Fabrication of Silk Fibroin Fluorescent Nanofibers via Electrospinning," Polymers, vol. 11, no. 6, pp. 986–986, Jun. 2019, doi: https://doi.org/10.3390/polym11060986.

[13] T. Yamane, Kôsuke Umemura, and T. Asakura, "The Structural Characteristics of *Bombyx mori* Silk Fibroin before Spinning As Studied with Molecular Dynamics Simulation," Macromolecules, vol. 35, no. 23, pp. 8831–8838, Oct. 2002, doi: https://doi.org/10.1021/ma0209390.

[14] J. Liu, T. Kong, and H. Xiong, "Mulberry-leaves-derived red-emissive carbon dots for feeding silkworms to produce brightly fluorescent silk," *Adv. Mater.*, p. 2200152, Mar. 2022, doi: 10.1002/adma.202200152.

[15] H. H. R. Ahmed, M. S. Saad, A. M. Abdel-Magid, M. F. Abdel-Attah, and M. A. M. Saad, "Assessment of use of some dyes for production of coloured silk from silkworm, *Bombyx mori* L. in Egypt," *Annals of Biology*, vol. 37, no. 2, pp. 201–208, 2021. [Online]. Available: https://www.researchgate.net/publication/362559035.

[16] N. Ramos, M. S. Miranda, A. R. Franco, S. S. Silva, J. Azevedo, I. R. Dias, R. L. Reis, C. Viegas, and M. E. Gomes, "Toward spinning greener advanced silk fibers by feeding silkworms with nanomaterials," *ACS Sustain. Chem. Eng.*, vol. 8, no. 32, pp. 11872–11887, 2020, doi: 10.1021/acssuschemeng.0c03874. [Online]. Available: https://pubs.acs.org/doi/10.1021/acssuschemeng.0c03874.

[17] N. C. Tansil *et al.*, "Intrinsically colored and luminescent silk," *Advanced Materials*, vol. 23, no. 12, pp. 1463–1466, Feb. 2011, doi: https://doi.org/10.1002/adma.201003860.

[18] N. C. Tansil *et al.*, "The use of molecular fluorescent markers to monitor absorption and distribution of xenobiotics in a silkworm model," *Biomaterials*, vol. 32, no. 36, pp. 9576–9583, Dec. 2011, doi: https://doi.org/10.1016/j.biomaterials.2011.08.081.

[19] J. Gu, "MilliFlex: A Multi-legged Millirobot with pH-Responsive Polymers for Targeted Drug Delivery," 2024 IEEE 3rd International Conference on Computing and Machine Intelligence (ICMI), Mt Pleasant, MI, USA, 2024, pp. 1-5, doi: 10.1109/ICMI60790.2024.10586038.

[20] D. Pratticò et al., "Integration of LSTM and U-Net models for monitoring electrical absorption with a system of sensors and electronic circuits," IEEE Transactions on Instrumentation and Measurement, pp. 1–1, Jan. 2025, doi: https://doi.org/10.1109/tim.2025.3573363.